Bidirectional Tests on Two Shaft-Grouted Barrette Piles in Mekong Delta, Vietnam

H. M. Nguyen[1], B. H. Fellenius[2], A. J. Puppala[3], P. Aravind[4], and Q. T. Tran[5]
[1]*PhD Student, Dept. of Civil Engng., Univ. of Texas at Arlington, TX 76019, USA*
[2]*Consulting Engineer, 2475 Rothesay Avenue, Sidney, BC, V8L 2B9*
[3]*Professor, Dept. of Civil Engng., Univ. of Texas at Arlington, TX 76019, USA*
[4]*Research Associate, Dept. of Civil Engng., Univ. of Texas at Arlington, TX 76019, USA*
[5]*Dept. of Civil Engng., Da Nang College of Technology, Da Nang, Vietnam*
[1]*E-mail*: haitdmu@gmail.com
[2]*E-mail*: bengt@fellenius.net
[3]*E-mail*: anand@uta.edu
[4]*E-mail*: pedarla@uta.edu
[5]*E-mail*: thquang2005@yahoo.com

ABSTRACT: The piled foundation design of the 40-storey Exim Bank Building in Ho Chi Minh City, Vietnam, included bidirectional static loading tests on two shaft-grouted barrette piles tested in September 2013. The soil profile consisted of organic soft clay on silty sand with some gravel and silty clay. The cross-section area of the barrette piles, TP1 and TP2, was 2,800 mm by 800 mm. They were excavated to 65-m and 85-m depth, respectively, using grab-bucket excavation techniques with bentonite slurry and guide wall advanced ahead of the hole. For each pile, the bidirectional cell assembly was installed 16 m above the pile toe level and the reinforcing cage was instrumented with diametrically opposed vibrating wire strain-gages at three levels below and five (TP1) to eight (TP2) levels above the cell level. Shaft grouting was carried out along a 40-m length above the TP1 pile toe and along a 20-m length above the TP2 pile toe. The static loading tests were performed 23 and 25 days, respectively, after the piles had been concreted. Analysis of strain-gage records indicated Young's modulus values of about 27 GPa on the nominal cross section of the piles. Simulation of the measured load-movement response indicated that the shaft resistance response was hyperbolic. The test schedule was interrupted by unloading/reloading cycles, which disturbed the gage data and included uneven load-holding durations which exacerbated the analysis difficulty.

KEYWORDS: Bidirectional tests, Barrette piles, Shaft grouting, Analysis of strain-gage records

1. INTRODUCTION AND BACKGROUND

The purpose of this paper is to illustrate the process of analysis of large instrumented bored piles and to compare the shaft resistance of a grouted shaft to a not-grouted shaft.

In recent years, the shaft grouting of deep drilled piles constructed to support high-rise building foundations has become common in Vietnam. Field studies related to improvement of shaft resistance in sand using post grouting technique were reported by Bolognese and Amoretto (1973), Bruce (1986), and Nguyen and Fellenius (2015). Up to three-fold improvement in shear resistance was observed for pressure-grouted shafts over not-grouted shafts. The case history reported by Nguyen and Fellenius (2015) is particularly relevant as it was comprised of tests on piles of similar size and depth as in the current case history and located as close as about 6 km (Figure 1).

Suthan et al. (2010) conducted large-scale laboratory tests in sand to study the influence of soil gradation, density, overburden stress, and grouting methods on the shaft resistance. Test results indicated increase in resistance with low mobility compaction grout. Littlechild et al. (2000) reported that shaft resistance measured for shaft-grouted barrettes and bored piles in completely weathered granite and volcanic soil achieved a two- to three-fold increase over results of tests without shaft grouting.

This paper examines the results from two test piles constructed for the Exim Bank Building, an approximately 163 m tall, 40 storey building in Ho Chi Minh City, Vietnam. The soil profile consisted of an about 90 m thick deposit of deltaic alluvial soils dominated by sand. When constructed, the building will include five basement levels, have a 3,520 m^2 foot-print area and a 25-MN sustained working load per pile. Before finalizing the piled foundation design, two barrette-type test piles, TP1 and TP2, were constructed and tested by means of bidirectional static loading test (Osterberg 1998). The test piles had a rectangular cross-section area of 2,800 mm by 800 mm. (The equivalent diameter of a circular pile is 1,680 mm and the equivalent diameter of a pile with the same circumference is 2,300 mm). The test piles were constructed to 65 and 85 m depth, respectively using grab-bucket excavation techniques with bentonite slurry. Each test pile had a bidirectional cell assembly placed about 16 m above the pile toe and the reinforcing cages were instrumented with several pairs of diametrically opposed vibrating wire strain-gages. Shaft grouting was carried out on both barrette piles after completion of concrete placement over about 40 m (TP1) and 20 m (TP2) lengths, respectively, above toe level. The purpose of the loading tests was to compare the response to load of not-grouted and grouted shafts.

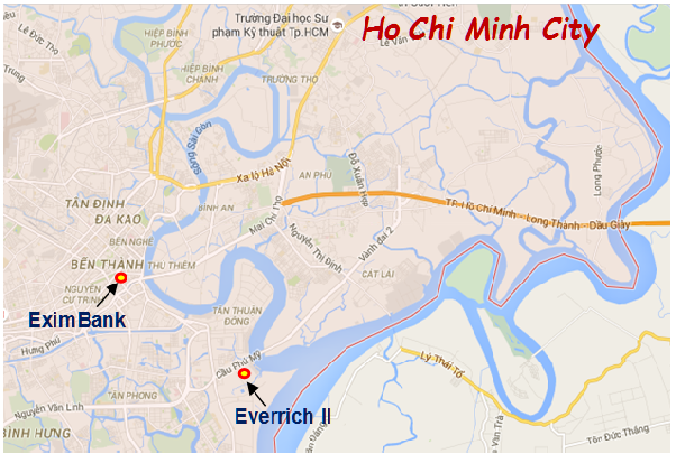

Figure 1 Ho Chi Minh City area with the meandering Saigon River and the locations of the Everrich II (Nguyen and Fellenius 2015) and Exim Bank sites

This paper presents the pile installation, the shaft grouting details, strain-gage evaluations, shaft resistance distributions, and correlations derived from the results of the tests with respect to the site conditions. Critical views are presented on the particular procedure chosen for the static loading test.

2. SOIL CONDITIONS

The soils at the site are typical for the Mekong Delta basin which is filled in with deposits from the Mekong River and consist of thick deposit of alternating alluvial soil layers of organic soft clay, compact silty sand with some gravels, and medium dense to dense silty sand, underlain by dense to very dense silty sand (Workman 1977). Regional settlements occur in the area. Figure 1 shows a map over the area with the locations of the subject Exim Bank project and the mentioned similar project, the Everrich II 37 storey apartment buildings site (Nguyen and Fellenius 2015), located about 6 km away. The map also shows the Saigon River, which meanderings established the upper soil layers of the city and the two sites.

The soil profile at the Exim Bank site consisted of soft clay to about 7 m depth on compacted alluvial sand with some gravel to 40 m depth followed by a 12 m thick interspersed layer of clay and silt. Hereunder, the soil profile consisted of old alluvium of medium dense to dense sand with some gravel to 78 m depth underlain by dense sand interspersed with trace clay and trace silt to 84 m depth followed by very dense sand with some gravel to at least 90 m depth. The site investigation included eight boreholes at locations shown in Figure 2. Figure 3 shows the distribution of water content, consistency limits, grain-size distribution, and SPT N-indices determined from the borehole records. The average saturated density and water content of the clay were about 1,800 kg/m^3 and 40 %, respectively. The average density of the sand was about 2,100 kg/m^3.

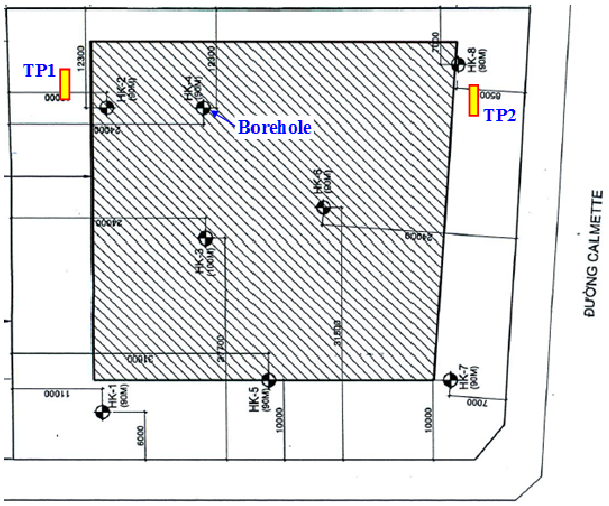

Figure 2 Layout of boreholes and test piles, TP1 and TP2

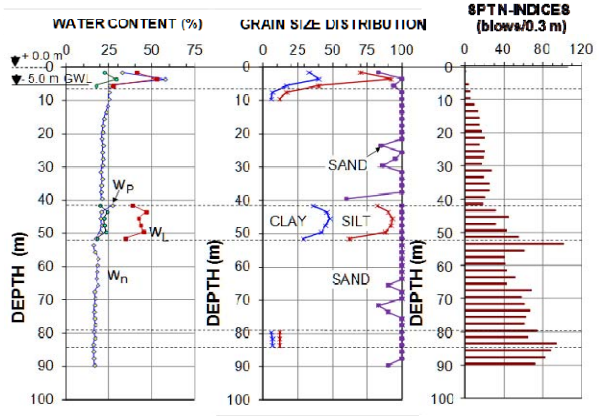

Figure 3 Water content, grain size distribution, and N-indices

The pore pressure distribution was hydrostatic and corresponded to a groundwater table at 5 m depth below the ground surface. From about 10 m through 40 m depths, the SPT N-indices increased from about 10 blows/0.3 m to about 18 blows/0.3m, indicating compact condition. Below 40 m depth, the N-indices showed the conditions to be very dense.

3. CONSTRUCTION OF TEST PILES

The two barrette test piles were constructed using rope grab excavation techniques with bentonite slurry. The construction was commenced by first constructing 300 mm thick, 1.5 m deep reinforced concrete guide walls with rectangular footprint equal to the barrette dimensions, to guide the excavator ("the grab") and to stabilize the ground around the shaft, as well as to support lowering the reinforcement cage and placing concrete. The excavation was then carried out using a rectangular grab operated by a crawler crane until the designed pile depth was reached. Bentonite slurry was used to support and maintain the hole.

The bentonite slurry properties monitored after completed excavation for both piles indicated a density of 1,080 kg/m^3, 38-s Marsh viscosity, pH of 9, and final maximum sand content of 1.0%. Before lowering the reinforcing cage and placing concrete, each shaft was cleaned by clamshell grab during recycling of the bentonite slurry.

Piles TP1 and TP2 were drilled on August 27 and August 30, 2013, to 65.3 m and 85.3 m depth below ground surface, respectively. Thereafter, the reinforcing cages with the bidirectional assembly attached at 16.8 m and 15.7 m above the pile toe level, respectively, were lowered into the stabilized hole, and concrete was poured through a 300 mm O.D. tremie pipe to the bottom of the shaft, displacing the bentonite slurry until the concrete reached the ground surface.

The concreting was performed and completed on August 30 and September 1, 2013, respectively. The average 21-day concrete strengths of Piles TP1 and TP2 were about 52 and 57 MPa, respectively.

Figure 4 shows for each test pile the locations of the vibrating wire strain-gages attached to the reinforcing cages (three levels below and five through eight levels above the bidirectional cell level). Each gage level (GL) contained two diametrically opposed pairs, Gages A and C, and Gages B and D, respectively. Additionally, Figure 3 also indicates the cut-off level of the construction piles at 25 m depth below the ground surface, i.e., depth of the future lowest basement level. The planners of the static loading test programme had decided to eliminate influence of the shaft resistance above this depth and, therefore, the test piles were constructed inside debonding steel-liners that were first coated with bitumen and, then, wrapped in geotextile and again coated with bitumen to minimize shear forces between the pile and the soil. The construction (working) piles were to be supplied with a temporary casing to 25 m depth and only concreted below that depth.

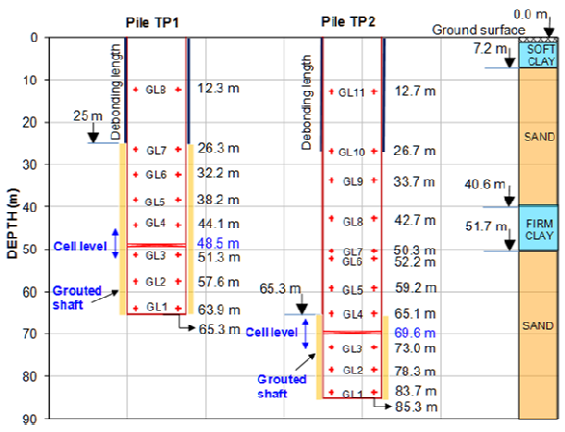

Figure 4 Details of grouting and instrumentation

Figure 5 shows the orientation of the reinforcement bars, telltales, strain-gages, and grouting tubes over the cross-section of the piles (the same arrangement was used for both piles). The piles were supplied with a reinforcing cage of thirty-six 32-mm bars, resulting in a steel reinforcement area of 289 cm^2 and a reinforcement ratio of 1.29 % for the 2.24 m^2 nominal pile cross section.

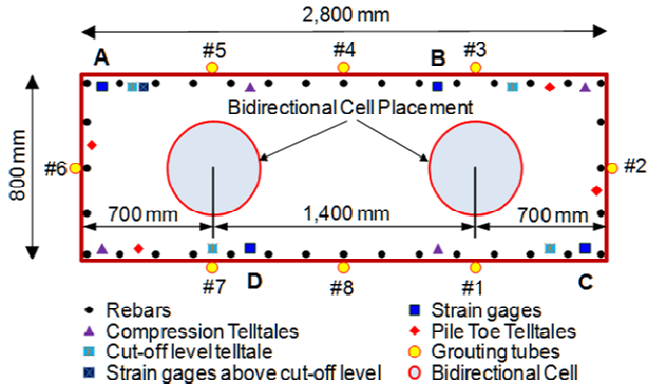

Figure 5 Cross section and layout of instrumentation

To arrange and facilitate the shaft grouting of the piles, eight 60-mm diameter pipes were symmetrically attached around the perimeter of the reinforcing cage throughout the shaft length. The concrete cover outside the grout pipe was 15 mm thick. Over the lower 40 m and 20 m length of Pile TP1 and TP2, the pipes were perforated for grout release and covered by a tight-fitting rubber sleeve. Grouting was carried out by means of inserting a "Tubes-à-Manchette" grouting tube with packers ("manchettes") that allow the grouting to be directed to a specific length (2.0 m) of the grout pipe at a time.

The strain-gages were placed diametrically opposed in pairs (gage pairs A & C and B & D), but because of the rectangular shape of the barrettes (Figure 5), the pairs did not cover equal areas of the barrette cross section. That would have meant placing the gages either at each barrette corner or at mid-point of each side (i.e., at grout tube locations #2 & #6 and #4 & #8, respectively). The actual placement indicates a quasi-symmetry across the barrette center for the gage pairs as placed..

Five days after placing the concrete, the shaft grouting was implemented by first cracking the pile concrete cover by pumping high pressure water through the grout tubes. The fact that the cracking of the concrete cover had been accomplished was signaled by a sudden drop of the water pressure occurring at 4,000-kPa pump pressure for both piles. The water was then turned off and cement grout was pumped down through the grout pipe expelling the water and forcing the grout out into the soil immediately outside the piles. The maximum grout pressures at the grout pump were 3,500 kPa and 3,200 kPa for Pile TP1 and TP2, respectively. A water-cement ratio of 1:2 was used for all grouting mixtures. The total grout volumes for pile TP1 and TP2 were about 11.2 m^3 and 5.6 m^3, respectively. Assumed to spread evenly along the pile perimeter, these volumes indicated an about 80 mm thick grout zone. Theoretically, adding this grout zone evenly to the pile circumference and area means a 4-% increase of circumference and a 13-% increase of pile cross section area.

4. ANALYSIS OF TEST RESULTS

4.1 Load versus Movement

The bidirectional loading tests for both piles were carried out in two loading cycles for both test piles (Loadtest Pte. Ltd. (2013). Figure 6 shows the load vs. time schedule. The Cycle 1 loading for both piles was performed by means of a first load-increment of 3.53 and 3.87 MN, respectively, followed by seven increments ranging from about 1.38 through 1.70 MN to a maximum load of 14.25 and 14.93 MN, respectively. The test piles were unloaded in four steps. Each of the first seven load increments of Cycle 1 was held constant during one hour and the 8th was held for 24 hours. In Cycle 2, the piles were first reloaded to the same 14.25 and 14.93-MN loads in four increments, whereafter the loading continued in ten and nine additional increments ranging from about 1.38 through 1.73 MN until a maximum load of 29.82 and 29.11 MN, respectively.

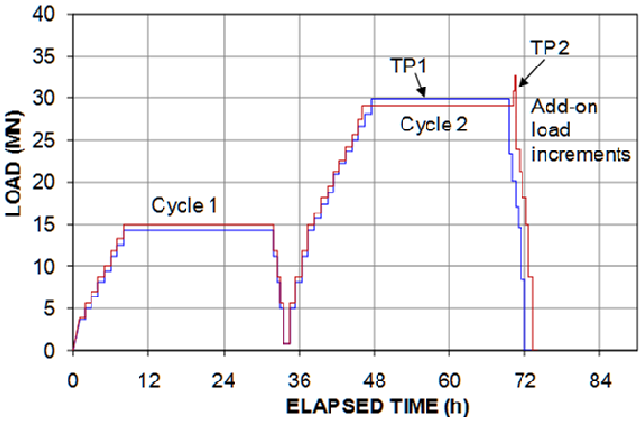

Figure 6 Loading schedule for the bidirectional assemblies placed 16.0 m above the pile toe and at 49 and 69 m depth for Piles, TP1 and TP2, respectively

All load levels were maintained for 60 minutes, but for Levels 10 and 13, which loads were held for 24 hours. For Pile TP2, two additional load increments of 1.73 MN held for 10 minutes were added after the last long-duration load-holding of Cycle 2 to a maximum load of 32.56 MN before unloading in seven steps.

It should be noted that the unloading and reloading and long load-holding imposed on the subject tests is regrettable because such interruptions of the test progress greatly impair the consistency of the strain-gage measurements, while providing no benefit whatsoever to the information to be gained from the test. The uneven magnitude of load increments and varying load-holding durations were additional sources of disturbance.

Figure 7 shows the measured upward and downward load-movement curves of the TP1 and TP2 bidirectional tests. Loads are those measured and are not adjusted for pile weight and water pressure at the cell level. At the end of the 60-minute hold for the maximum load, the Pile TP1 and TP2 Cycle 2 downward cell movements were 9.0 mm and 5.9 mm, the toe movements were 4.6 and 2.2 mm, the upward cell movements were 6.7 and 6.9 mm, and the pile head movements were 1.2 and 0.8 mm, respectively. For TP2, the change of the downward load-movement curve to becoming less steep after the unloading and reloading event is probably due to some disturbance to the dial gages. For both piles, the initially very small movements for increasing load were probably due to the piles being affected by some residual load.

4.2 Strain Gage Measurements

Strain measurements in piles must always be in pairs placed diametrically opposed. If so, the average strain will offset any bending effect—be representative for true axial strain. The records of both gages in the pair are needed. If one gage of the pair becomes unreliable, the value of the "surviving" gage of the pair will be in question and the records of the "surviving" gage should be discarded. It is, therefore, advisable to schedule two gage pairs to important levels in the test pile. Having two gage pairs will also improve the representativeness of the measurements because some variation of stress from one side of the pile to the other is unavoidable. In a cylindrical pile, four gages placed symmetrically around the pile perimeter may individually show different values, but the two gage-pair averages can be expected to be similar.

The quasi-symmetrical (A, B, C, and D) placement of the gages, as opposed to symmetrically around a circular shape, was found to produce different averages, but most gages or gage pairs appeared to provide reasonable values. The exceptions were Gage Pair B-D at Gage Level 4 in TP1 and all Gage Level 4 gages in TP2, as addressed below. The unloading-reloading cycle in the midst of each test introduced a major disturbance for the evaluation of the gage records.

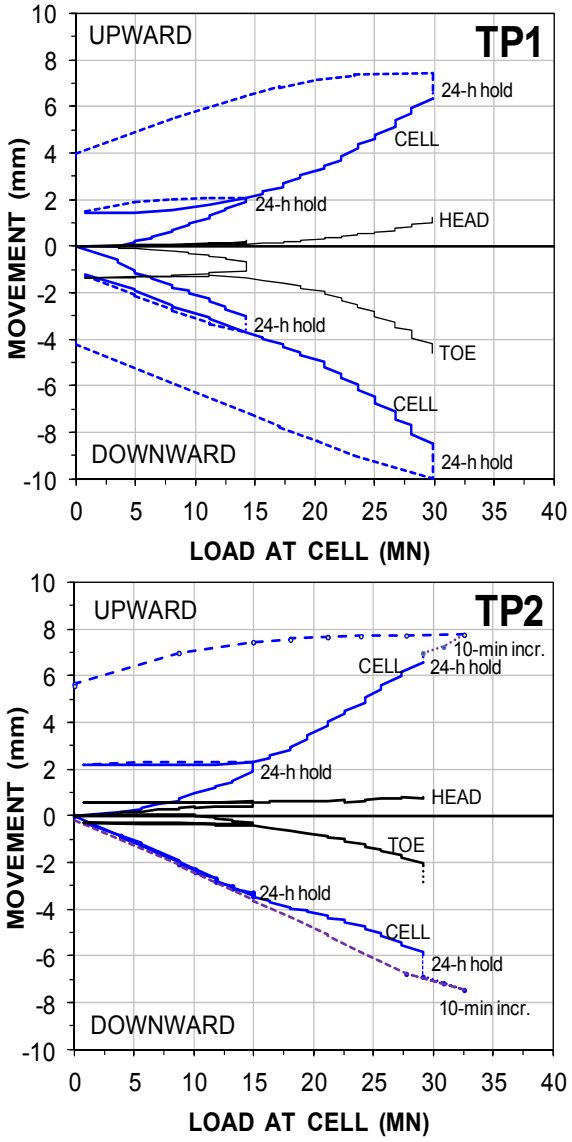

Figure 7 Measured load-movement curves

Pile TP1. Figures 8 and 9 show the TP1 load vs. strain recorded at Gage Levels 3 and 4 for Cycles 1 and 2, respectively. The individual gage records are plotted as continuous lines and the average of each gage pair is plotted as a dashed line. For TP1 Gage Level 3, three of the gage records (A, B, and C) are very similar, whereas the fourth (D) deviates from the others. Possibly, the GL3D is "off" but there is no other indication of suspect data in the gage records than the divergence. The Gage GL3(B+D) records were therefore not discarded. In contrast, Gage Level 4 records show a similar scatter of all four gage records: the gage-pair averages (Gage Pairs A+C and B+D) differ at each gage level. The maximum difference between the two averages is about 200 με. The scatter in Level 4 records is due to GL4D appears to have ceased to work properly and GL4(B+D) records were therefore discarded. The other TP1 gage levels, GL1, GL2, GL5, GL6, GL7, and GL8 (not shown here) appeared to functioning adequately and the averages of both gage pairs were considered representative for the axial strain measured at the respective levels.

Pile TP2. Figures 10 and 11 show the TP2 load vs. strain recorded at Gage Levels 3 and 4 for Cycles 1 and 2, respectively. The individually measured GL3 strains differ slightly. However, the

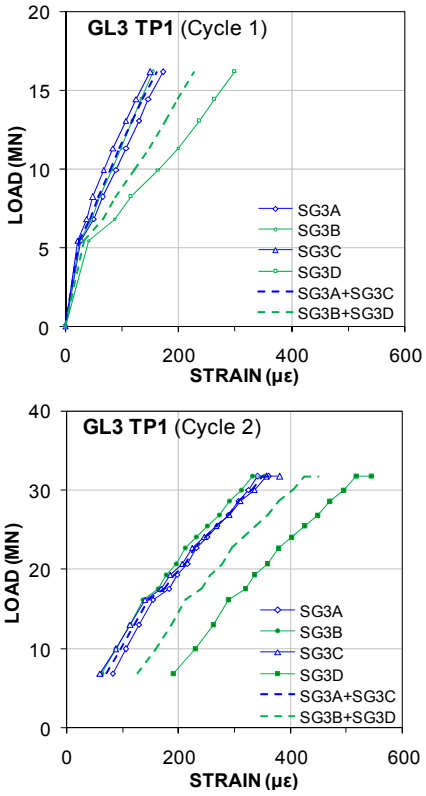

Figure 8 Load-strain measured at Level 3 (51.3 m) of TP1

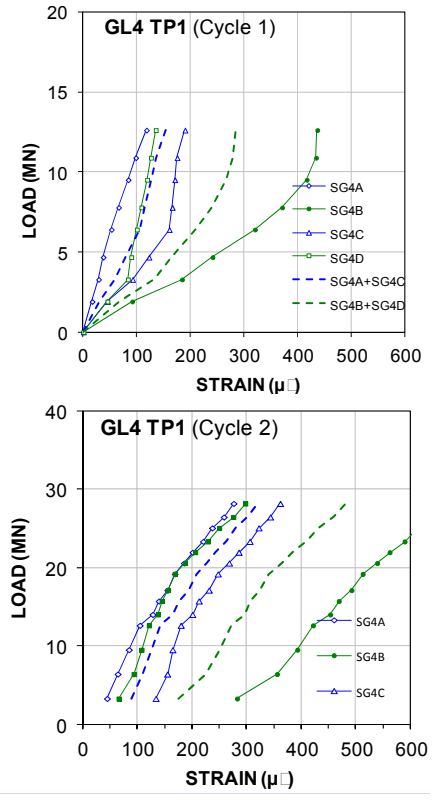

Figure 9 Load-strain measured at Level 4 (44.1 m) of TP1

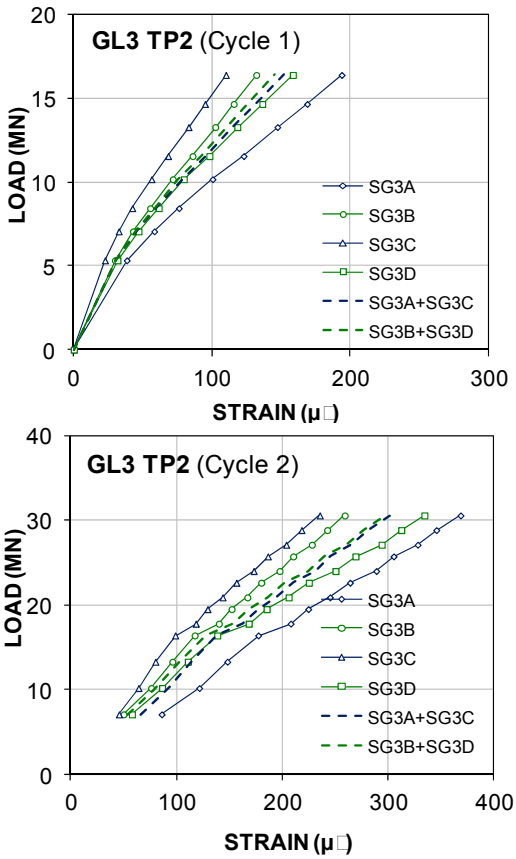

Figure 10 Load-strain measured at Level 3 (51.3 m) of TP1

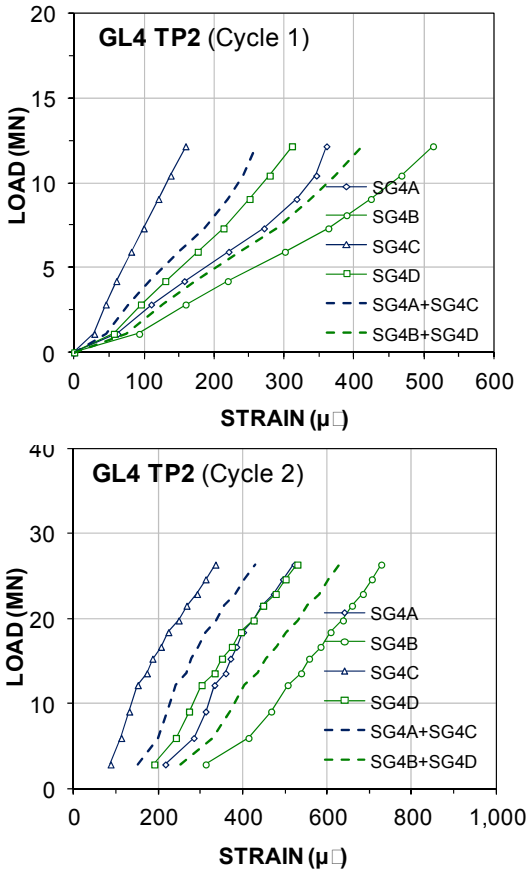

Figure 11 Load-strain measured at Level 4 (44.1 m) of TP1

average of the GL3 (A+C) pair is very close to the average of the GL3 (B+D) pair. As in TP1, the records from Gage Level 4 show a scatter. The maximum difference between the two averages is about 500 με. All gage values from GL4 were considered suspect and were therefore discarded. The records from all other gage levels were considered to function satisfactorily and the average strain was considered representative of the axial strain response.

Figures 12 and 13 combine the average strains records for the two load cycles applied to TP1 and TP2, respectively. As is usually the case, the load-strain relations are slightly curved, which is due to the influence of shaft resistance and, but to a minor degree, to the fact that concrete modulus reduces with increasing strain. Short portions of the curves will always appear rather straight, however.

The average slope of the curve—once the relative movement between the pile and the soil at the gage level is large enough for the shaft resistance to become fully mobilized—will indicate, approximately, the stiffness of the pile (provided that the continued shear force development is neither strain-hardening nor strain-softening to any significant degree). Therefore, the slope of that portion of the curve will be the pile stiffness, EA, as a function of strain as determined by a linear regression analysis (Fellenius 2015).

Thus, at the movement magnitude at GL3 (TP1 and TP2) and GL4 (TP1) toward the end of Cycle 2, the slope of the end of the curves may represent the pile stiffness. The slopes were 73 and 79 GN for TP1 GL3 and TP1 GL4, respectively, and 95 GN for TP2 GL3. However, these stiffness values are larger than usually established in similar tests in the area (e.g., Nguyen and Fellenius 2015), as will be discussed below.

The best way of determining the pile modulus is by means of a so-called "tangent modulus" or "incremental stiffness" plot (Fellenius 1989; 2015), that is, the applied increment of load over the induced increment of strain plotted versus the measured strain. Figure 14 shows the incremental stiffness plot for the gage levels nearest the bidirectional cell levels for the test piles. The maximum strains, about 350 to 400 με induced by the applied loads are smaller than ideal. (Ideally, the maximum strains should have been at least 600 με for the final stiffness to be established accurately and also to establish the strain dependency of the stiffness). The several millimetre relative movement between the pile and the soil would normally have mobilized an ultimate shaft resistance ("plastic" shear) in the Cycle 2 tests. Therefore, the shaft shear is expected to be more or less fully mobilized between the bidirectional cell and GL3 and GL4, and GL4 to GL5 of both test piles. This could be the case also along the lengths between GL2 and GL3 and GL4, and between GL5 and GL6. However, each load-increase resulted in increased shaft shear and the implied stiffness values are too high.

This response is typical for a strain-hardening behavior, as opposed to an ultimate "plastic" shear-force vs. movement response. Moreover, the trend shown for TP1 beyond 300 με is increasing, as opposed to decreasing. This suggests that the pile shaft surface was corrugated. Possibly, outside each grout hole in the grout pipes the grout zone is thicker than between the grout hole levels. Thus, the grouting has created a series of more or less horizontal ribs or "donuts" that act as displacement-depended "toe resistances" in building up resistance to the pile movement, much in similarity to undereamed piles or step-taper piles (Fellenius 2015). Thus, for the first few millimetre of movement, the resistance is mainly shaft shear. Then, at larger movement, when the shaft shear approaches its ultimate value—although, there may or may not be an ultimate shaft shear resistance—due to deformation similar to toe resistance, the latter response takes over, resulting in an apparent increase of the incremental stiffness.

The actual stiffness was not evident from the records. Judging from other similar tests in the general area, the end stiffness is reasonably about 60 GN, which corresponds to a Young modulus of about 27 GPa on the nominal cross section. It is not possible to use the data to deduce a strain-dependent stiffness toward the 60-GN end value. Therefore, all strain data are evaluated for the 60-GN value, which somewhat underestimates the axial force in the pile at small strains.

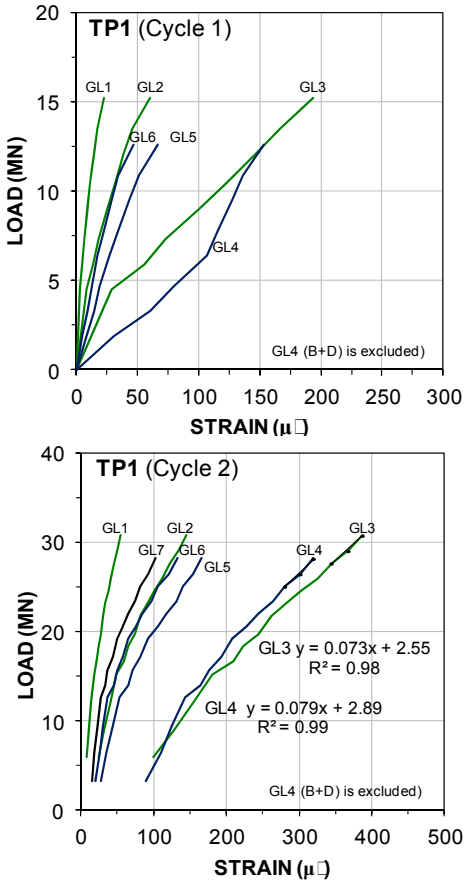

Figure 12 Bidirectional cell load versus measured strain for TP1 Cycles 1 and 2

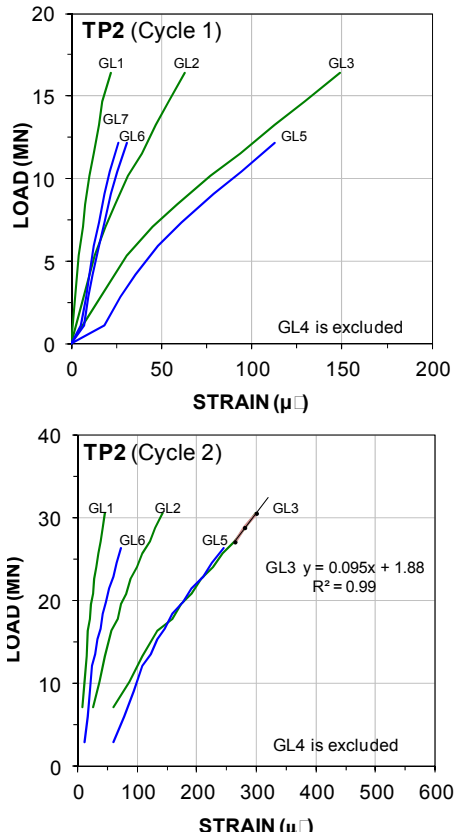

Figure 13 Bidirectional cell load versus measured strain for TP2 Cycles 1 and 2

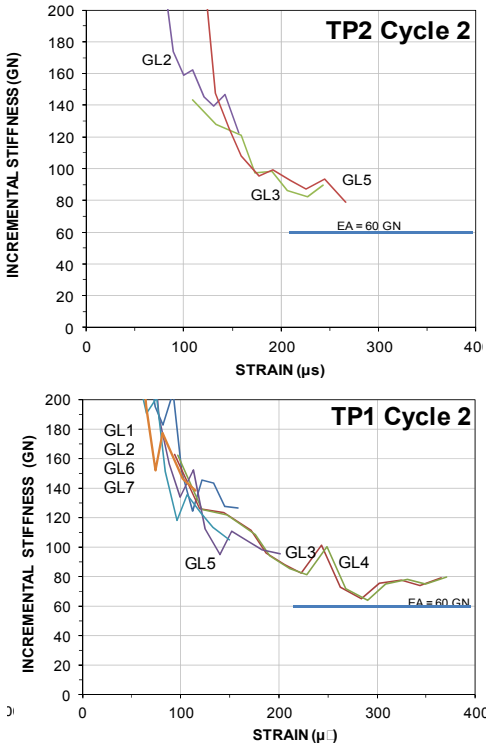

Figure 14 Load-strain measured at Level 3 (51.3 m) of TP1

4.3 Load Distributions along the Pile Shafts

The derived 60-GN pile stiffness was used to convert the average of strain measured at each gage level for each applied load. The results for the two tests are shown in Figures 15 and 16, respectively. The lines of loads plotted above the cell level connect to the respective cell loads minus the buoyant pile weight above the cell level and the lines below connect to a respective cell loads plus the load resulting from the water pressure at the cell level. No consideration of residual load was included.

The even distributions indicated that the chosen 60-GN stiffness is a reasonable stiffness to use for the back-calculation of the load distribution. A larger stiffness would have resulted in load magnitudes at GL3 and GL4 (TP1) and GL3 and GL5 (TP2) too close to the applied cell loads, or even larger than the cell loads. This would only have been possible if the pile had micro-cracks before the start of the test, which is improbable. Micro-cracks may develop in rock sockets, where the shaft shear is able to prevent the concrete from reducing volume (height) during the cooling after the hydration process and, thus, develop cracks, but that does not apply here. Or, the pile could have been subjected to residual (locked-in) loads which then would have had to be caused by positive shaft shear above the cell level and negative shaft shear below. Presence of such locked-in loads is highly unlikely, indeed impossible, as it would have required the soils to have undergone swelling. Above the cell level, presence of residual load would have resulted in strain-gage evaluated loads that are smaller than the true loads.

4.4 Toe Resistance versus Movement

For both piles, the lowest gages, GL1, was located very close to the pile toe. Figure 17 shows the GL1-load vs. the telltale-measured pile toe movement. The Pile TP2 toe movement showed a sudden sideways shift at the end of the test that, probably, was due to some unknown incidence affecting the movement readings. Both curves were fitted to a q-z function curve shown with dashed lines per the ratio function (Fellenius 2015) according to Eq. 1.

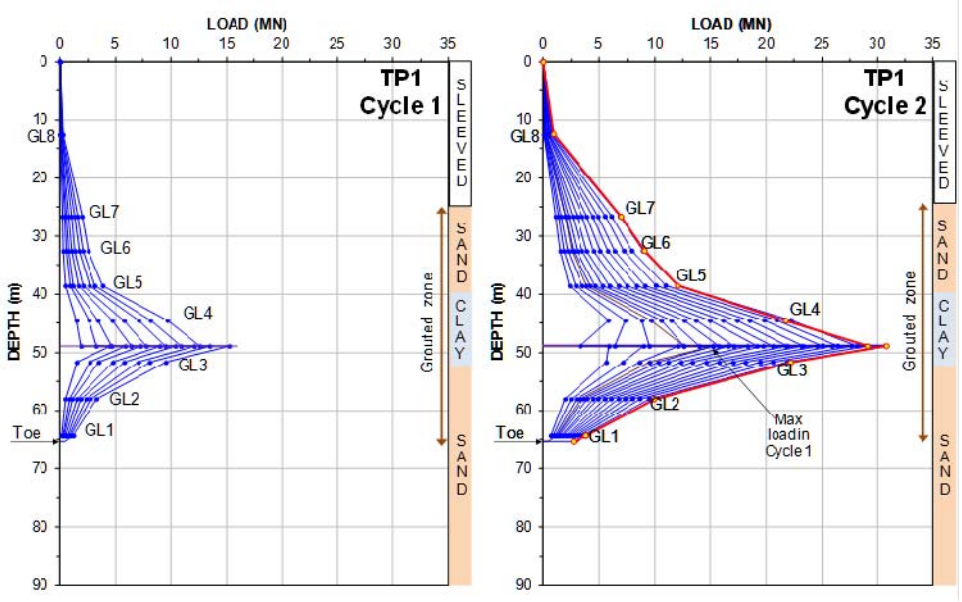

Figure 15 TP1 Cycles 1 and 2 load distributions

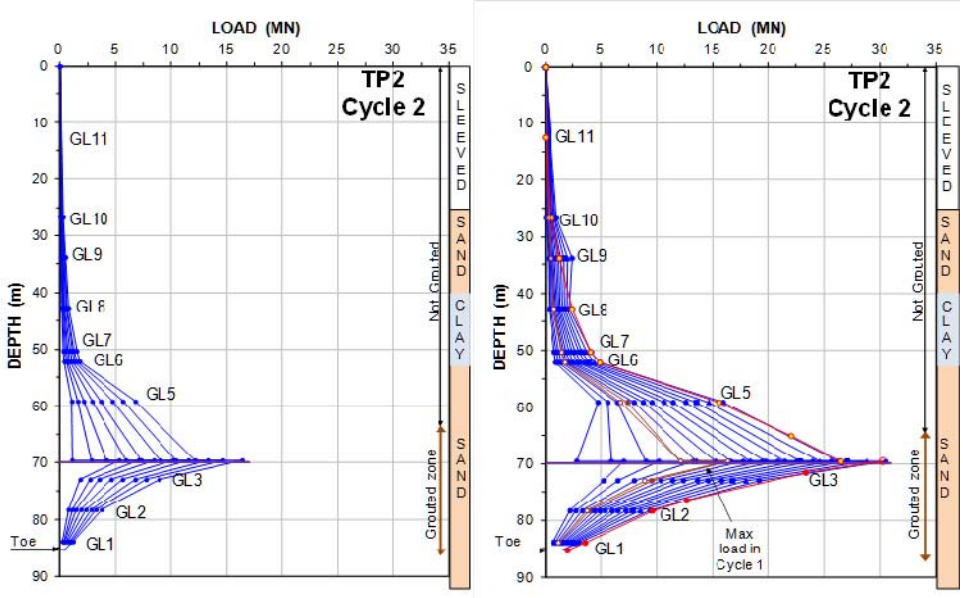

Figure 16 TP2 Cycles 1 and 2 load distributions

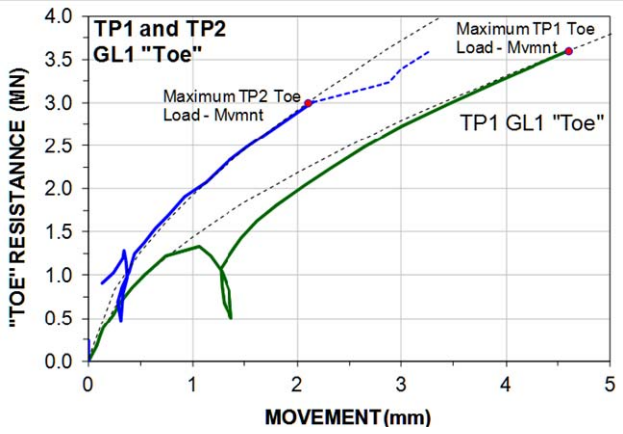

Figure 17 Gage Level 1 in Piles TP1 and TP2 vs. telltale-measured pile-toe movements and q-z fits for the Ratio Function with the θ-exponents equal to 0.6

$$\frac{R_{trg}}{R_n} = \left(\frac{\delta_{trg}}{\delta_n}\right)^{\theta} \tag{1}$$

where R_{trg} = Reference or target resistance
R_n = Any resistance
δ_{trg} = Movement mobilized for R_{trg}
δ_n = Movement mobilized for R_n
θ = an exponent; $0 \le \theta \le 1$

Thus, when assigning any load/movement point as the R_{trg}/δ_{trg}, any and all other load-movement pairs are determined by the θ-exponent. As mentioned below, a θ-exponent equal to 0.6 was found to provide a toe load-movement curve that fitted the measured response for both piles.

4.5 Shaft Shear Resistance versus Movement

The difference in load between the gage levels is the shaft resistance between the pile and the soil. Dividing the resistance with the pile circumference times the distance between the two gage levels considered, produces the average unit shaft resistance between the gage levels. Figures 18 and 19 show the so-calculated shaft-shear vs. movement for the gage levels of Pile TP1 and TP2, respectively. It should be noted that this differentiation process can result in uncertain unit shaft resistance values because the error (inaccuracy) of each load value can be large in relation to the difference between the load values. This makes the differentiation results prone to include large relative errors.

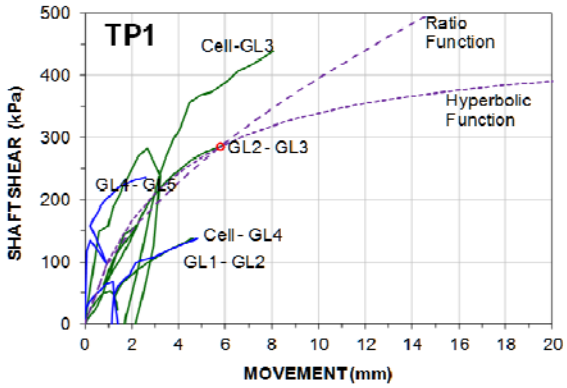

Figure 18 Pile TP1 shaft shear vs. movement in Cycles 1 and 2 with curves fitted per Ratio and Hyperbolic t-z Functions

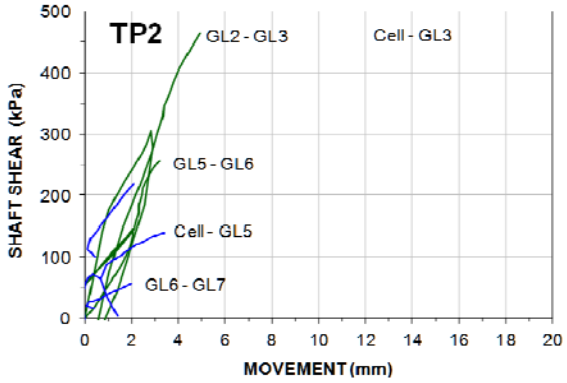

Figure 19 Pile TP2 shaft shear vs. movement in Cycles 1 and 2

The pile movements were measured at cell level and the pile toe. The movements at GL4 and GL3 above and below the cell level, were calculated as the upward and downward movement, respectively, measured at the cell level minus the average of strain time the distance to the strain gage level. The movements at the next gage levels above and below were calculated with respect to the movements at GL4 and GL3, respectively, and so on for the next level. (As mentioned, the TP2 GL4 records were considered unreliable and were, therefore, not used, which means that Figure 19 does not include curves for Cell-GL4 and GL4-GL5). The movement induced in the test were rather small and, with the possible exception for the pile lengths immediately above and below the cell level, the shaft resistance was not fully mobilized.

The Ratio Function showed to fit the curves for a □-exponent ranging from 0.4 through 0.6, as demonstrated by the fit to the average shear resistance between TP1 GL2-GL3 using a □ exponent equal to 0.60 (Figure 18). However, because the movements are small, a suitable fit can also be found for any other t-z functions that show an increase of resistance for increasing movement. For example, the hyperbolic fit (Fellenius 2015) as expressed by Eqs. 2 and 3.

$$R_n = \frac{\delta_n}{\frac{\delta_n}{R_{\text{inf}}} + C_2} \tag{2}$$

where R_n = Any resistance
δ_n = Movement mobilized for R_n
R_{inf} = Resistance at infinite movement
R_{trg} = Reference or target resistance
δ_{trg} = Movement mobilized for R_{trg}
C2 = y-intercept or slope of curve at zero movement;

$$C_2 = \delta_{trg}\left(\frac{1}{R_{trg}} - \frac{1}{R_{\text{inf}}}\right) \tag{3}$$

Within the initial movements up to the maximum value either function provided an acceptable fit. However, at larger movements, the t-z functions deviate considerably.

Usually, the Hyperbolic Function is more representative for the mobilization of shaft resistance as opposed to the Ratio Function. The results from the Everrich II tests, which was carried out to much larger movement, suggested that this was the case for the Everich II site. Figure 20 shows the unit shaft shear vs. movement for one of the Everrich II test piles. Both the Ratio and Hyperbolic t-z Functions have been fitted to the Cell-GL1 shear force vs. movement curve. The functions provide a good fit to the initial part of the curve. However, for large movement, the Ratio Function overestimated the shear force, whereas the Hyperbolic Function keeps providing a good fit.

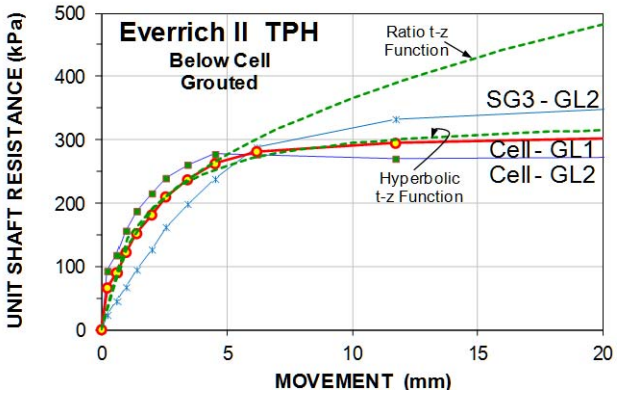

Figure 20 Unit shaft resistances vs. movement determined for the Everrich II test. The TPH pile was a 2,000-mm diameter, 80 m long bored pile (data from Nguyen and Fellenius 2015)

4.6 Simulating the test by t-z and q-z functions

The basic measurements in a bidirectional test are the load and movement at the cell level and the pile head and the telltale-measured movement of the pile toe. (The load at the pile head is always zero, a very accurate and useful load value for analysis reference). Strain-gage instrumentation, when included in the test, provides a second rank of values. Simulation of the bidirectional test measurement is thus rather simple, as the response of the portions above and below the cell level can be modeled separately from each other: the length above the cell level is affected by shaft shear, only, and the toe response movement can be treated separately from the shaft shear along the lower length. In a multi-layered soil, the process can still be quite complex. However, for the subject case of three individually rather coherent soil layers—sand to clay to sand—the process is straight-forward, as the shaft shear can be considered uniform within each layer. NB., as in all

meaningful analysis of shaft response of a test pile, the shaft shear "uniformity" lies within the restrictions of the effective overburden stress.

The software UniPile5 (Goudreault and Fellenius 2014) was employed to a simulate the TP1 and TP2 load distribution and measured load-movements. The primary simulation input was the description of the pile in terms of pile geometry, pile unit weight, and pile Young's modulus, the soil unit weight, the groundwater level, and thee pore pressure distribution. The first simulation effort consisted of fitting beta-coefficients that resulted in a calculated axial load distribution equal to the loads determined from the strain-gage records at the gage levels as measured for the 10-minute measurements of the last load applied. For the toe resistance, similarly, the toe resistance at the toe movement for the 10-minute measurements of the last load applied was calculated by extrapolation of the trend of axial load calculated from the strain-gage values, notably, the closest gage, GL1. The calculated distribution has been added to the load distribution curves for Cycles 2, in Figures 15 and 16, respectively, as the line representing the 10-minute measurements of the last load applied.

The simulation of the load-movements consisted of fitting the calculated upward and downward and the toe movement curves to the measured curves for the applied cell loads. For the toe resistance, the target TP1 and TP2 points were applied to a Ratio q-z Function with the θ-exponent equal to 0.6. Indeed, it is rare not to see an increase of resistance with increasing movement, i.e., a "strain-hardening" response, similar to the toe resistance Ratio Function. For shaft resistance, however, other functions are usually possible.

For analysis of shaft response, it is necessary to select beta-coefficients and movement at the 10 minute measurements of the last load applied and combine these with the specific t-z function. The beta-coefficients used were those obtained by fitting the analysis to the back-calculated load distribution. Each such load value, called "target load", was then assigned a movements equal to the measured movement at cell level, pile toe, and pile head, as adjusted with pile shortening estimated from the measured strains. The analysis was carried out for a series of 1.0 m long pile elements.

As mentioned, the strain-gage determined load-movements indicated that also the shaft shear response was "strain-hardening". Of the several functions (Fellenius 2015) that can be used to model a shaft load-movement response, only the Hyperbolic Function and the Ratio Function provide increasing resistance with increasing movement. While they can be produced to show similar shapes at small movement, the hyperbolic function shows a more depressed increase for large movements, as opposed to the ratio function. For the subject test, the target beta-coefficients and movements were then combined with either a θ-exponent (Ratio Function) or a resistance, R_{inf}, at infinite movement (Hyperbolic Function). The simulation of the bidirectional test was then carried out for different such parameters until a satisfactory fit was achieved. Both t z functions produced equally good fits to the measured load-movement curves, as shown in Figures 21 and 22.

Table 1 columns show the input of movement and beta-coefficients used for the UniPile simulation and the R_{inf} resistance that gave the fit shown in the figures. The table also includes the calculated effective overburden stress and the unit shaft resistance at the gage levels as corresponding to the beta-coefficient times the effective stress.

Table 1 Movements at gage levels and back-calculated beta-coefficients

Gage Level	Depth (m)	Mvmnt (mm)	ß (--)	σ'z (kPa)	rs (kPa)	
TP1						
Head	0	1.2				
GL9	12.6	1.1	0.03	176	5	
GL8	26.6	1.2	0.04	317	13	grouted
GL7	38.5	1.5	0.08	316	25	grouted
GL6	32.6	1.8	0.20	375	75	grouted
GL5	38.5	3.5	0.25	435	109	grouted
GL4	44.5	5.0	0.52	486	253	grouted
Cell	48.9	↑6.7 ↓9.0				
GL3	51.7	7.6	0.80	544	435	grouted
GL2	58.0	5.4	0.47	610	287	grouted
GL1	64.3	4.6	0.21	676	142	grouted
Toe	65.3	4.6	0.21	θ = 0.6		
TP2						
Head	0	0.8				
GL11	12.7	0.8				
GL10	26.7	0.9				
GL9	33.7	0.7	0.03	387	12	
GL8	42.7	0.8	0.04	472	19	
GL7	50.3	1.5	0.06	316	25	
GL6	52.2	2.0	0.11	375	30	
GL5	59.2	2.8	0.37	435	109	
GL4	65.1	5.3	0.25	486	253	grouted
Cell	69.6	↑6.9 ↓5.9				
GL3	73.0	5.5	0.66	544	435	grouted
GL2	78.3	4.0	0.30	610	287	grouted
GL1	83.9	2.3	0.18	676	142	grouted
Toe	85.3	2.2	0.18	θ =0.6		

The beta-coefficients and movements are those determined in the test at the 10-minute measurements of the last load applied—the target point. They are not the ultimate resistance values.

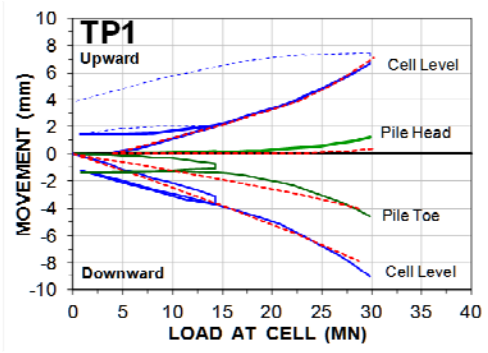

Figure 21 TP1 Measured and load-movement curves. Solid lines show the measured curves and dashed lines the simulated curves

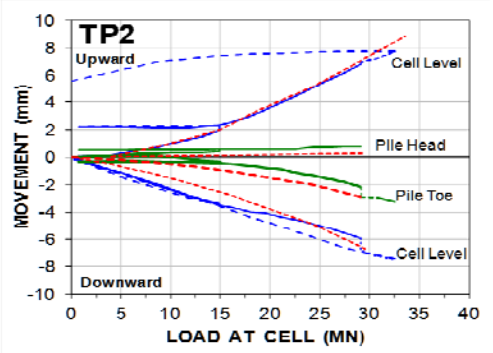

Figure 22 TP2 Measured and load-movement curves. Solid lines show the measured curves and dashed lines the simulated curves

4.7 Effect of grouting

A primary objective of the test was to compare the shaft shear response for a grouted length to that of a non-grouted length. It is however very difficult to discern any clear difference in shaft response between the pile lengths that were grouted (Pile TP1) and not grouted (Pile TP2). The comparison needs to be for gage lengths at equal depths and over pile elements that more or less have mobilized most of the shaft resistance, or at least have been moved an equal distance relative to the soil. This limits the comparison to using the grouted lengths in TP1 to below GL4 and, for Pile TP2, to no-grout lengths between TP2 GL5 and GL7 (TP2 GL4 records were discarded). The shaft shear above TP2 GL7 was not mobilized to a useful degree. The shaft-shear curves suitable for such comparison must be from approximately same depth range. Curves relevant for comparison are assembled in Figure 23. Only one record along a no-grout pile length applies, TP2 GL5-GL6 (the dashed curve). The curves from the length between TP1 cell and GL3 mobilized considerably larger shear force compared to the TP2 GL5-GL6 no-grout length. However, grout-length curves TP1 GL2-GL3 and GL1-GL2, as well as TP1 Cell-GL4 did not show larger shaft shear than the TP2 GL5-GL6 no-grout gage length at similar depth range.Judging by the strain-hardening resistance, the indication is that the grouting increased the shaft shear, but the records plotted in Figure 20 are not definite enough to serve as base for a quantified comparison.

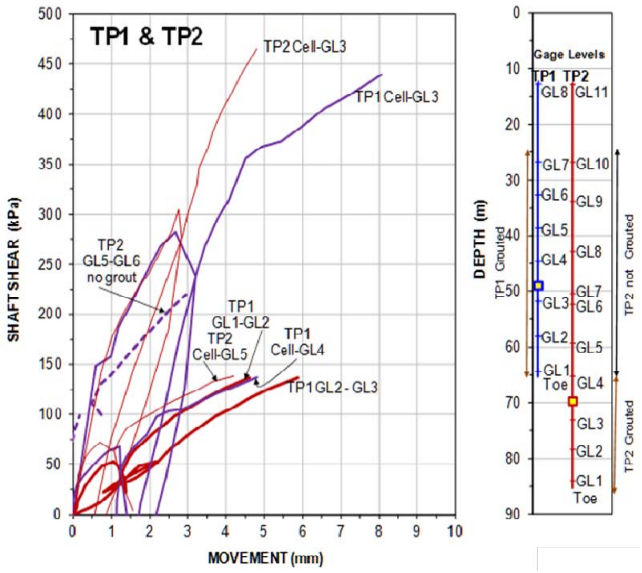

Figure 23 Comparison of shaft shear vs. shaft movement for grouted and not grouted pile lengths between gage levels

When comparing values for grouted and non grouted lengths, only values for GL5 to GL3 in TP1 and the same depth range values GL8 to GL6 in TP2 apply. In TP1, the beta-coefficient ranges from 0.43 to 0.99; the average was 0.71. In TP2, the range was 0.11 to 0.40; the average was 0.21. This appears to indicate that the grouting did indeed result in an increased shaft resistance and, possibly, one as large as that found in the tests mentioned in the introduction, specifically at the Everrich II test (Figure 20).

It is likely that continuing the test beyond the 32.6-MN maximum cell load and avoiding the unloading and reloading cycles and extra load-holding would have provided more conclusive records. It is regrettable that this was not brought about—extending to test to loads beyond 32.6 MN could have been achieved without incurring any additional costs.

It is simple to extrapolate the simulation to movements (and load) beyond those of the actual test; however, the two t-z functions then produce very different results. The experience of the Everrich II tests indicate that an extrapolation analysis using the hyperbolic function, as fitted to the test, would result in the more probable result. Such extrapolations are often performed to show an equivalent head-down test load-distribution or a equivalent head-down load-movement curve. They are of interest in bidirectional test that are carried to larger movements than the current one. However, although a simulation is easily performed, it would not be realistic here.

A head-down test simulation using UniPile on Pile TP1 with the input of the parameters obtained by the fitting of the test records shows that the pile head would have to move more than 30 mm before any load would reach the pile toe. To engage the pile toe to the same movement as in the bidirectional test would require applying a pile head load in excess of 100 MN. The two test piles are vastly overdesigned for the desired 25-MN working load.

The construction of the piled foundations for the project was delayed and has not yet commenced. The authors hope that the design will be based on a smaller and shorter pile. The current records can be used in the selection of the new pile. The design should consider the effect of the planned excavation of the site, not just in discounting any shaft resistance in the excavation, but also the unloading effect in terms of reduced effective stress along the piles below the excavation. Moreover, although the excavation will have an unloading effect, the area is subject to ongoing regional subsidence and settlement should be an important issue in the design. One or two new preconstruction bidirectional tests will be necessary. It is hoped that they will be designed without any unloading-reloading cycles and extra load-holding duration so that the test records are not impaired. Finally, when the intended maximum test load is reached, the test should continue until either the limit of the cell expansion movement or the capacity of the cell is reached, so as to obtain maximum information for the evaluation of the test results.

5. CONCLUSIONS

The Exim Bank Tower project test piles were overdesigned as to size and depth in respect to the intended working load. Consequently, the maximum test loads were rather limited and the induced strains were smaller than desirable for the analysis of the test data. The unloading/reloading cycle interruption of the test disturbed the gage data and the uneven load-holding durations exacerbated the difficulty in analyzing the test results.

The detailed analysis of the measured loads, movements, and strains were fitted to simulated results showing the shaft resistance to be increasing with increasing movement. Applying the ratio and hyperbolic t-z functions showed that the actual test data could be fitted equally well to either function, which is due to the fact that the movements imposed in the tests were very small. However, comparison to results from similar tests in the area, which had been performed to larger movements, suggested that the hyperbolic t-z function is the most appropriate for the shaft resistance simulation.

The test results indicate that the intended working load can be supported on smaller and shorter piles subject to a settlement analysis. Such change in design will have to be confirmed in additional, well-designed, static loading tests.

6. ACKNOWLEDGEMENTS

The authors wish to thank Mr. Huynh Thanh Vinh, deputy site manager of the Exim Bank project, for permission to use the project data.

7. REFERENCES

Bolognesi, A.J.L., and Moretto, O., 1973.Stage grouting preloading of large piles on sand. Proc., 8th ICSMFE, , August 12-19, Moscow, Vol. 2.1, pp. 19-25.

Bruce, D. A. 1986. Enhancing the performance of large diameter piles by grouting, Parts 1 and 2, Ground Engng., 19(4) 7 and 19(5) 7.

Fellenius, B.H., 1989. Tangent modulus of piles determined from strain data. ASCE, Geotechnical Engineering Division, the 1989 Foundation Congress, F.H. Kulhawy, Editor, Vol. 1, pp. 500-510.

Fellenius, B.H., 2015. Basics of foundation design, a text book. Revised Electronic Ed., [www.Fellenius.net], 432 p.

Goudreault, P.A. and Fellenius, B.H., 2014. UniPile Version 5, User and Examples Manual. UniSoft Geotechnical Solutions Ltd. [www.UniSoftLtd.com]. 120 p.

Littlechild, B., Plumbridge, G., Hill, S., and Lee, S. (2000) Shaft Grouting of Deep Foundations in Hong Kong. New Technological and Design Developments in Deep Foundations: pp. 33 45.

Loadtest International Pte. Ltd., 2013. Reports on Barrette Pile Testing, Exim Bank Tower, HCMC, Vietnam, 13813I-1 and 13813I-2,178 p and 133 p.

Nguyen, H.M. and Fellenius, B.H., 2015. Bidirectional cell tests on non-grouted and grouted large-diameter bored piles. Journal of Geo-Engineering Sciences, IOS Press, 2(3-4) 105-117.

Osterberg, J.O., 1998. The Osterberg load test method for drilled shaft and driven piles. The first ten years. 7th Int. Conf. on Piling and Deep Foundations, Deep Foundation Institute, Vienna, Austria, June 15-17, 17 p.

Suthan P, Sherif E., Walt V., and Gray N., 2010. Large scale laboratory testing of low mobility compaction grouts for drilled shafts tips ASTM Geotechnical Testing Journal, 33(5) 13.

Workman, D.R., 1977. Geology of Laos, Cambodia, South Vietnam, and the eastern part of Thailand. Overseas geology and mineral resources, 50, Her Majesty's Stationery Office, London, 33 p.